Photosynthesis Research (2020) 143:335–346
https://doi.org/10.1007/s11120-020-00712-3

ORIGINAL ARTICLE

Variable fluorescence of closed photochemical reaction centers

Agu Laisk[1] · **Vello Oja**[1]

Received: 5 September 2019 / Accepted: 13 January 2020 / Published online: 21 January 2020

Abstract

Chlorophyll fluorescence induction during 0.4 to 200 ms multiple-turnover pulses (MTP) was measured in parallel with O_2 evolution induced by the MTP light. Additionally, a saturating single-turnover flash (STF) was applied at the end of each MTP and the total MTP + STF O_2 evolution was measured. Quantum yield of O_2 evolution during the MTP transients was calculated and related to the number of open PSII centers, found from the STF O_2 evolution. Proportionality between the number of open PSII and their running photochemical activity showed the quantum yield of open PSII remained constant independent of the closure of adjacent centers. During the induction, total fluorescence was partitioned between F_o of all the open centers and F_c of all the closed centers. The fluorescence yield of a closed center was 0.55 of the final F_m while less than a half of the centers were closed, but later increased, approaching F_m to the end of the induction. In the framework of the antenna/radical pair equilibrium model, the collective rise of the fluorescence of centers closed earlier during the induction is explained by an electric field, facilitating return of excitation energy from the $Pheo^-$ $P680^+$ radical pair to the antenna.

Keywords Photosynthesis · Leaves · Chlorophyll fluorescence

Abbreviations

Chl	Chlorophyll
ETR	Electron transport rate
FI	Fluorescence induction
F_{max}	Fluorescence yield from the antenna
F_m,	Maximum fluorescence yield at the end of a saturation pulse
F_f	Fluorescence yield after a single-turnover flash
F_c	Running fluorescence yield of a closed center
FR	Far-red light
LHCII	Light-harvesting complex II
MTP	Multiple-turnover pulse
PFD, PAD	Photon flux density, incident and absorbed
Pheo	Pheophytin
PQ	Plastoquinone
PSI, PSII	Photosystem I and photosystem II
P680	Six-Chl complex in reaction center
Q_A	Primary quinone acceptor of PSII
Q_B	Secondary quinone acceptor of PSII
RP	Radical pair
STF	Single-turnover flash
ΔE	Voltage difference

Introduction

When leaves are illuminated with strong light of the intensity of about 2–3 sunlight, Chl fluorescence initially rapidly increases during a few ms, but then stops on about a halfway and continues to increase with a slower rate—until it approaches the maximum F_m yield at about 200 ms (Schansker et al. 2011; Laisk and Oja 2018). Under ultrastrong microseconds-long xenon flashes of the intensity of a thousand sunlight Chl fluorescence reaches about the same level as during the first milliseconds under the lower light, but the additional rise to F_m does not happen (Joliot and Joliot 1964; Neubauer and Schreiber 1987; Samson and Bruce 1996). These two cases differ by the final state: the ST flash-induced induction ends with reduced Q_A, but oxidized Q_B and the rest of the ETC. The pulse-induced induction ends with the full reduction of Q_A, Q_B and the whole electron transport chain. This fact has induced a notion about a "thermal phase" of fluorescence rise, caused by release of a hypothetical quencher while ETC is being reduced (Delosme 1967; Schreiber and Neubauer 1987; Neubauer and Schreiber 1987; Koblížek et al. 2001; Vredenberg

✉ Agu Laisk
agu.laisk@ut.ee

[1] Institute of Technology, University of Tartu, Nooruse st. 1, 50411 Tartu, Estonia

et al. 2009; Stirbet and Govindjee 2012). Multiple potential quenchers have been suggested (Vredenberg 2008; Stirbet and Govindjee 2012; Koblížek et al. 2001): (1) $P680^+$ can quench Chl a fluorescence as efficiently as Q_A reduction; (2) P680 triplet, $^3P680$, most likely $^3Chl_{D1}$ quenches in equilibrium with $^3P_{D1}$; (3) carotenoid triplet ^3Car is an efficient quencher in the antenna; (4) non-photochemical quenching by oxidized PQ molecules; (5) quenching by charge recombination from Q_B (Schreiber 2002); (6) reduced $Pheo_{D1}$ may be a quencher due to charge separation equilibrium $P680^* \leftrightarrow P680^+Pheo^-$, shifted by transmembrane electric field (photo-electrochemical quenching (Vredenberg et al. 2009); (7) quenching by conformational changes in Chl proteins (Schansker et al. 2011); (8) fast recombination of separated charges in a cycle involving oxidized tyrosine Z (Laisk and Oja 2018). Contrary to the latter, (Prášil et al. 2018) showed that in *Chlamydomonas reinhardtii* donor side was not involved, but F_m was low when the Q_B binding site was occupied by PQ, and high when it was empty or occupied by DCMU or by PQH_2.

Membrane energization by electric field as a factor controlling Chl fluorescence has been repeatedly emphasized (Schatz et al. 1987; Leibl et al. 1989; Keuper and Sauer 1989; Schreiber and Neubauer 1990; Schreiber and Krieger 1996; Vredenberg et al. 2009; Dau and Sauer 1992; Pospíšil and Dau 2002), but there is no direct evidence showing how the fluorescence yield of closed PSII centers is modulated by its presence. In the experimental part of this work, we first show that during low to high light induction, Chl fluorescence yield of closed reaction centers in sunflower leaves is not constantly F_m, but gradually increases, approaching the F_m value to the end of the induction. For explanation, we present a mathematical model similar to that of Schatz et al. (1988), but considering the repulsive force applied by an electric field on the radical pair. With this modification, the model predicts that the fluorescence yield of closed reaction centers increases during the induction, approaching the F_m level. According to this model, the ST flash-induced fluorescence level F_f is a fluorescence yield value, established in the state when Q_A has been reduced in most PSII, but the electric field, related to plastoquinone reduction and membrane energization, has not yet accumulated.

Materials and methods

Used leaves and measurement methods were essentially the same as those in (Laisk et al. 2012). Briefly, sunflower (*Helianthus annuus* L.) plants were grown in laboratory at a PFD of 450 µmol quanta m^{-2} s^{-1}. O_2 evolution was measured at 22 °C in the two-channel leaf gas exchange measurement system (Laisk et al. 2002), where the leaf was enclosed in a 32-mm diameter by 3-mm-deep chamber, flushed with gas at a flow rate 0.5 mmol s^{-1}. The leaf chamber was illuminated through a branched fiber-optic light guide, producing uniform illumination of the adaxial leaf surface from three superimposable light sources. One branch was connected to a 630-nm LED light source providing a PFD of up to 8200 µmol quanta m^{-2} s^{-1} on the leaf surface. The second branch was used for far-red (FR) illumination. The third branch was connected to a xenon lamp, producing flashes of 7 µs half-width, photon dose of 76.7 µmol m^{-2} on the leaf surface, which saturated flash-induced O_2 evolution. Leaf absorption was measured in a laboratory-made integrating sphere. Energy-calibrated actinic light spectra were measured by Miniature Fiber Optic Spectrophotometer PC2000 (Ocean Optic, Dunedin, FL). Photon fluence rate absorbed by the leaf in the photosynthetically active range was calculated as the product of the spectra of the incident light and leaf absorption from 400 to 700 nm. The red as well as FR light were integrated over their actual spectrum.

Oxygen evolution was measured in the flow-through system with a zirconium O_2 analyzer (S-3A, Ametek, Pittsburgh, PA, USA) on a background of 10–20 ppm O_2 in N_2 and 200 ppm CO_2. The MTP- and STF-induced O_2 evolution was recorded as a bell-shape peak of 0.6 s half-width (for details see Oja et al. 2010). Integral O_2 evolution from individual MTPs of gradually increasing length was approximated by a polynomial. Time-resolved ETR was calculated as four times the running slope of the polynomial. The rates are presented in µmol e^- m^{-2} s^{-1} and sums in µmol e^- m^{-2}. The total per area density of PSII centers capable of water splitting was measured as four times O_2 evolution from an individual saturating STF (Oja and Laisk 2000). Gradually decreasing density of open PSII centers during the induction was found by applying an STF at the end of MTPs of gradually increasing length. The difference in total O_2 evolution from (MTP + STF) − MTP characterized the number of open PSII.

Chlorophyll fluorescence was excited by the same 630 nm LED light source that provided actinic (MTP) illumination. The fluorescence signal was collected from a 2 cm^2 area of the leaf and recorded with a PIN diode sensor S3590-01 (Hamamatsu, Japan), whose signal was amplified by a THS 4601 chip connected to a laboratory-made DC amplifier (Oja et al. 2010). The sensor was protected from the excitation beam by a 750 ± 20 nm bandpass interference filter, a small cross-sensitivity signal was considered. The fluorescence excitation light was continuously recorded along with the fluorescence emission, using quantum sensor LI-190SA (LiCor, Lincoln, NE) connected to an amplifier. Fluorescence yield (in relative units) was calculated as the ratio of the fluorescence signal to the incident excitation intensity signal.

Results

Experimental approach

Before the application of MT pulses and ST flashes, leaves were stabilized under FR light, to keep the ET chain oxidized and S-states randomized due to the slow PSII excitation. Recorded fluorescence inductions (Fig. 1) began at the minimum value denoted F_o, but a little higher than the minimum fluorescence in the dark, rapidly increased during about 1 ms and then more slowly approached the maximum F_m level during the recording time of 300 ms.

O_2 evolution could be recorded integrally from MT pulses of different lengths. The FR light was turned off simultaneously with the pulses and flashes, which was reflected as a step down in the reference O_2 recording. Oxygen, evolved by the pulses and flashes, was superimposed on the reference transient (Fig. 2).

The sum of O_2 evolution induced by individual MT pulses of different photon dose was fitted by 6-th power polynomials (Fig. 3). The running O_2 evolution rate was found as analytical derivative (slope) of the polynomial and multiplied by four to be presented as ETR. As this O_2 evolution was produced by PSII still open during the induction, the rate reflects the quantum yield of all the PSII still open: the yield was maximal in the very beginning, but decreased towards saturation of the induction.

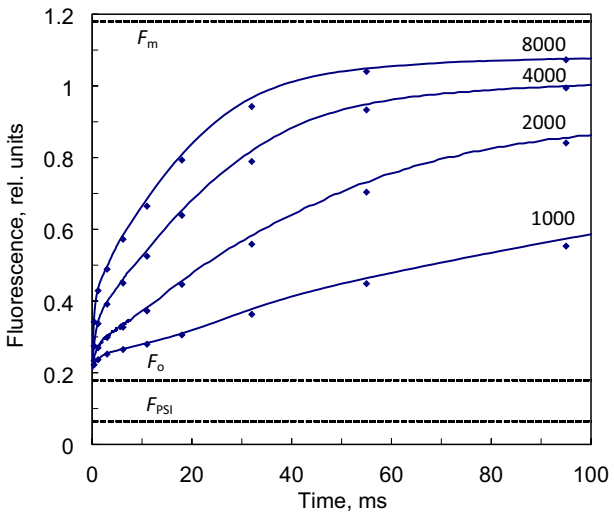

Fig. 1 Recorded fluorescence inductions (lines) at indicated light intensities (μmol m^{-2} s^{-1}). These recordings lasted 300 ms, but for clarity only the initial part is shown. For O_2 measurements, the pulses were repeated at length as indicated by data points. Each data point shows the actual fluorescence reached to this time moment in the particular recording. Dotted lines indicate F_m approached to the end of the recording (F_m is normalized to unity in figures below), F_o is the starting point of recordings (steady-state under low FRL), F_{PSI} is PSI fluorescence

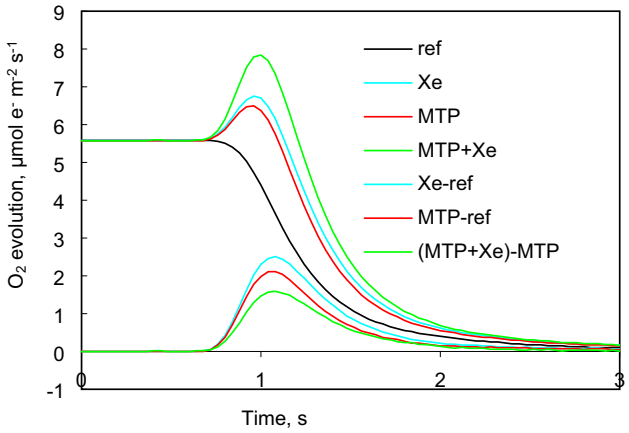

Fig. 2 Example of O_2 evolution measurements. A leaf was stabilized under FRL of 50 μmol m^{-2} s^{-1} to randomize S-states, activate ATP synthesis and carbon metabolism. The FRL-excited PSII generated steady-state O_2 evolution, equivalent to ETR of 5.6 μmol e^- m^{-2} s^{-1}. Light pulses and flashes were superimposed on this state, simultaneously FRL was turned off. The corresponding transients in O_2 evolution were measured and integrated. Denotations in the legend on the panel are the following: black (ref)—reference transient without pulsing; Xe (blue)—only xenon flash, inducing O_2 evolution from 1/4 of active PSII centers in the leaf; MTP (red)—multiple-turnover pulses of different lengths and intensity (the example is a weak MTP, exciting less than all PSII units); MTP + Xe – a xenon flash was added at the end of the MTP with an aim to measure the fraction of still open centers. Point-by-point differences between the traces resulted in the following information: Xe—ref (blue), total number of active PSII; MTP—ref, summary electron transport during the applied MTP; (MTP + Xe) – MTP, fraction of PSII still open after the MTP

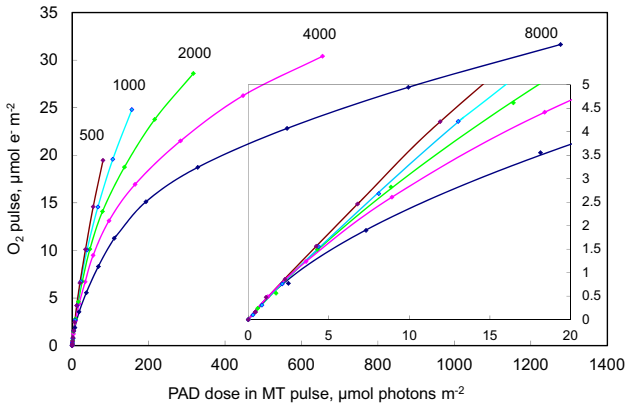

Fig. 3 O_2 pulses measured in response to MT light pulses of different intensity and length. Absorbed photon dose is on the abscissa, increasing as the pulse length was increased from 0.4 to 200 ms. Continuous lines are 6th power polynomials fitted to the data points. Different lines correspond to different PAD of the pulse light, indicated at the curves, μmol m^{-2} s^{-1}. Inset shows details in the initial part of the curves, emphasizing intensity-independent initial slope

The number of open PSII was derived from O_2 evolution induced by a saturating ST flash applied at the end of the actinic MT pulse. The number of open PSII was maximal in the beginning, but decreased towards saturation of the induction. When the summary yield (rate during the MT pulse) was plotted against the fractional number of open PSII, the result indicated proportionality independent of the way the photons were applied—either during an intense short pulse or weaker longer pulse (Fig. 4). This shows that open centers operated at a constant quantum yield independent of the density of adjacent closed centers.

Figure 5 represents the increasing fluorescence yield as measured from the leaf while the fraction of closed centers was growing during the induction. The curve begins at the minimum fluorescence slightly higher than the dark fluorescence of open centers F_o because of the slow excitation by FRL. Importantly, the curve is not linear—as expected assuming a constant F_m value for a closed center—but it curvilinearly increases as more PSII centers become closed. Proceeding from the fact that the quantum yield of open centers remained constant (Fig. 4), we assume that each open center keeps fluorescing at the initial yield during the whole induction. The blue line in Fig. 5 presents the decreasing summary fluorescence of open centers as their fraction decreases, being replaced by the growing fraction of closed centers. The final offset of the blue line characterizes PSI fluorescence (Peterson et al. 2014). This plot shows that fluorescence from closed PSII increases with an accelerating speed while more centers become closed during the induction.

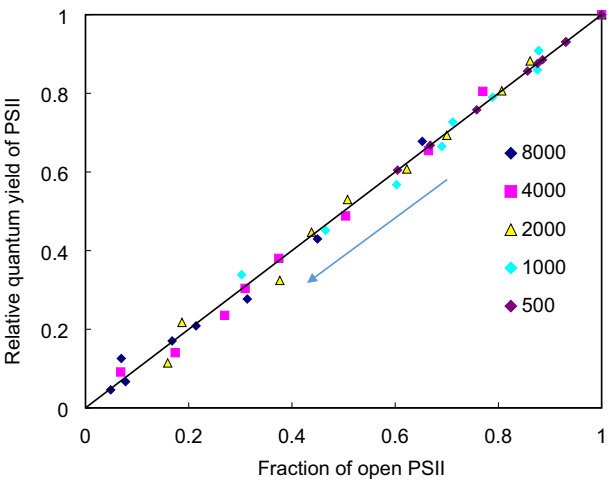

Fig. 4 Decreasing rate of electron transport, supported by the gradually decreasing fraction of open PSII during low–high light induction. Proportionality indicates a constant yield. Arrow indicates direction of the induction

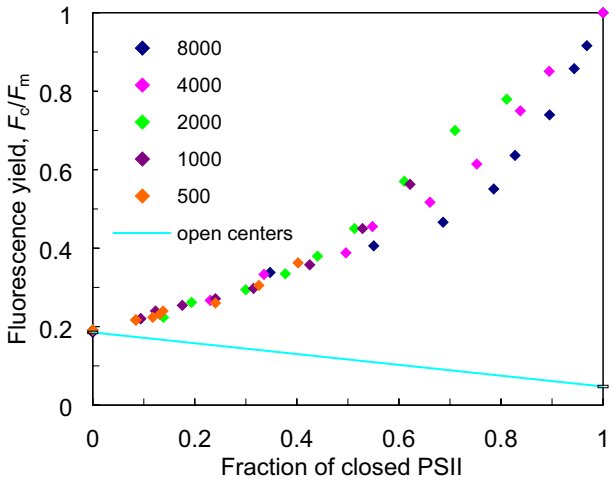

Fig. 5 Fluorescence yield during induction dependent on the fraction of closed PSII; color of data points indicates PAD. F_o is the summary fluorescence yield of open centers, linearly decreasing with the decreasing fraction of open centers (blue line, offset indicates PSI fluorescence)

In Fig. 6, the total fluorescence yield of all closed centers—difference between the data points and the blue line in Fig. 5—was divided by the fractional amount of closed centers, revealing the fluorescence yield of a closed PSII center. Regulation of the fluorescence yield of closed PSII centers is best visible in the Panel A, where the light intensity was the highest. While electrons were transferred to reduce Q_A and Q_B, but not yet many electrons were reducing plastoquinone and PSI donor and acceptor side carriers, fluorescence yield of a closed PSII F_c was 0.55 of the final level denoted F_m. This yield is close to F_f, the one usually obtained after a ST flash. The yield was constant until 70% of PSII became closed due to reduction of their bound quinone acceptors, but not many electrons were yet transferred to PQ and other carriers of ETC. Fluorescence yield of closed PSII centers gradually increased, approaching the final F_m level when the whole ETC became reduced. At lower pulse light intensities the fraction of centers closed before the PSII ETR equilibrated with the reduction rate of PQ was smaller—e.g. 30% at the pulse light intensity of 2000 µmol m^{-2} s^{-1} and less at the still lower light intensities. At physiological light intensities F_c did not approach the high F_m reached at 8000 µmol m^{-2} s^{-1} of pulse PFD. At the typical growth light of 500 µmol m^{-2} s^{-1} closed centers emitted at the flash fluorescence F_f level, not showing a tendency to increase fluorescence during the 200 ms pulse—but it does not mean that a longer exposure at this PFD could not cause enhancement of fluorescence.

Concluding this section, we have established that fluorescence yield of a PSII center getting closed by Q_A

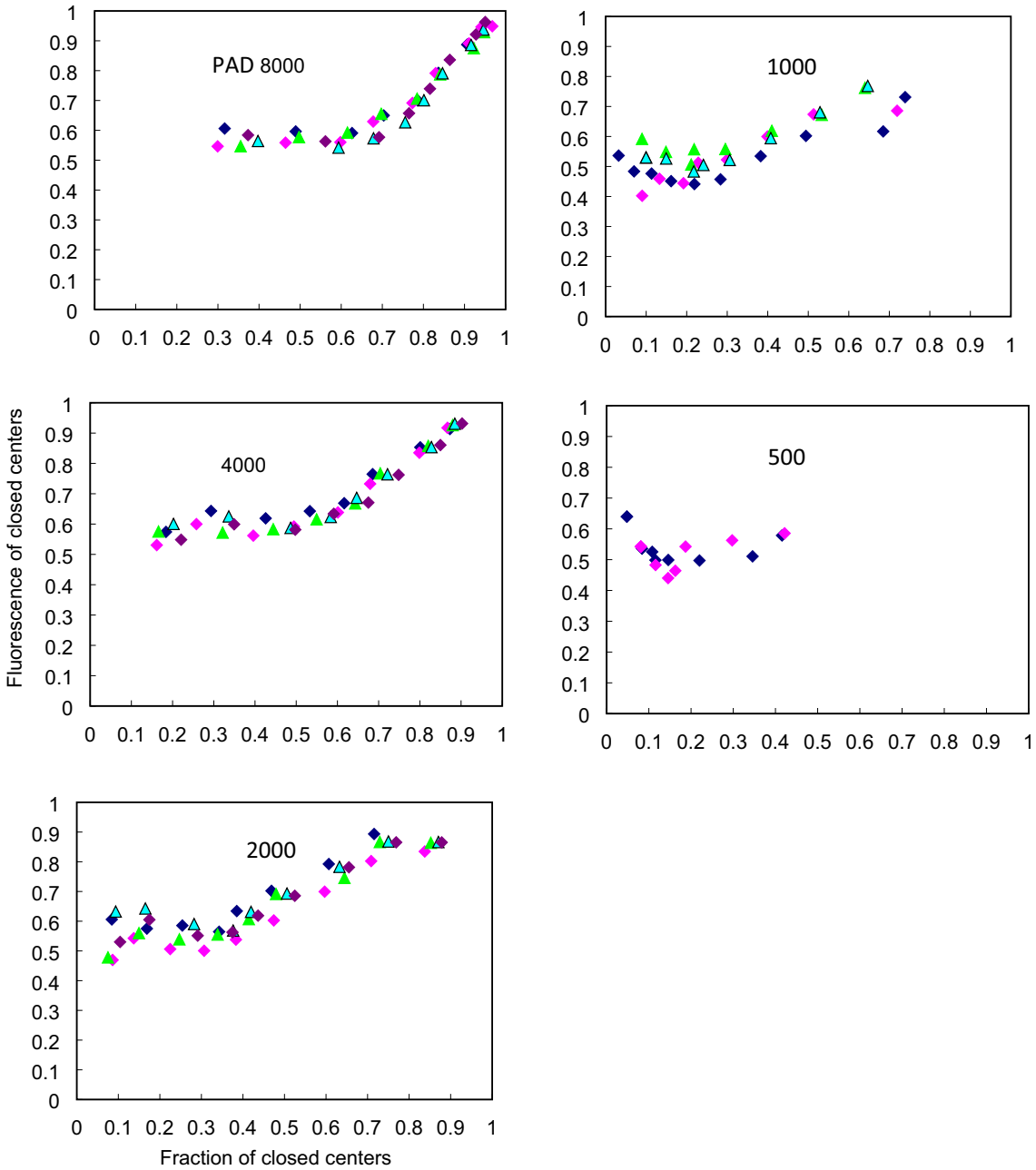

Fig. 6 Fluorescence yield of closed reaction centers, F_c in relation to $F_m = 1$, dependent on the fraction of closed reaction centers during induction. Fluorescence yield was close to the flash-induced $F_f = 0.55$ F_m while the acceptor side carriers Q_A and Q_B were being reduced, but started to increase as soon as the whole electron transport chain became to be reduced. Different symbols indicate results obtained with different sunflower leaves

reduction in the state of unrestricted electron transport is 3.7 F_o. In the state of restricted electron transport, the whole ET chain becomes reduced, generating an allosteric effector that gradually increases the fluorescence yield of all closed centers—*including those which had become closed earlier*—to 6.7F_o.

Modeling the variable PSII fluorescence emission

Here, we present a simple model to explain mechanistic principles of the variability of fluorescence yield of closed PSII centers. The model (Fig. 7) is similar to that used by A. Holzwarth and coworkers (Schatz et al. 1987, 1988; Szczepaniak et al. 2008, 2009; Lambrev et al. 2012). For leaves, however, the 6-Chl PSII reaction center complex is joined with the large antenna as in (Holzwarth et al. 2009; Lambrev et al. 2012). There are two sites terminating excitation in this model. While randomly hopping in the antenna, excitation may be terminated as fluorescence emission or as heat generated either by internal conversion in an antenna pigment or via an intermediate triplet state. The other chance to terminate it is while excitation is deposited in the radical pair. In open centers, the most likely pathway for this is photochemical charge transfer to Q_A, but if the latter happens to be reduced, then excitation may be terminated by non-radiative recombination or recombination via a triplet state (Lambrev et al. 2012). The probability for being terminated rises with the time excitation is spending as the radical pair. By elevating the energy level of the radical pair (decreasing the free-energy difference with the antenna), electric field controls relative efficiencies of the two excitation termination sites: when the field is weak, the radical pair is a deeper trap, where excitation spends a longer part of its lifetime, offering a good chance for the photochemical charge transfer in open centers, or for non-radiative charge recombination in closed centers. When the field is strong, excitation spends little time in the shallow trap of the radical pair, but spends most of its lifetime randomly hopping in the antenna—with this increasing the chance of being terminated via fluorescence emission. Only one radical pair state is considered in this model, denoted $Pheo^{-}P680^{+}$. With this we smooth the initial ultrafast kinetic effects discernable by separating RP_1 and RP_2 ($Pheo^{-}Chl_{accD1}^{+}$ and $Pheo^{-}P_{D1}^{+}$ Lambrev et al. 2012).

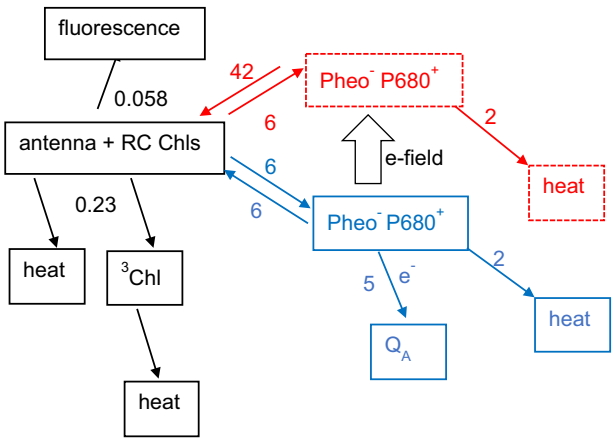

Fig. 7 Model of excitation transfer within a PSII. Initially excitation is located in the pigment system of antenna + RC (black boxes); from there it moves to the $Pheo^{-}P680^{+}$ radical pair; the latter may recombine to the ground or excited levels, or the electron may move further to Q_A (blue boxes). In energized membranes with closed centers (red boxes), electric field pushes the radical pair to return excitation energy to the antenna. Rate constants are given in ns^{-1}

Mathematical analysis was executed by solving a system of linear differential equations, describing transformations between the states of PSII with differently located excitation. As an initial condition, the antenna was excited. With time the excitation could move to form the radical pair and later to reduce Q_A, but the excitation could competitively be terminated while being in the antenna or in the radical pair. In equation denotations, the A(ntenna) R(adical)Q(uinone) complex could be in states with antenna in excited, Ae, or ground, Ag, radical pair present, AgRQo, or absent, AeQo, and the quinone acceptor oxidized AgRQo or reduced, AgQr. Rate constants characterizing transformations between these states were evaluated, considering well-measured integrals—such as the maximum fluorescence F_m and the minimum fluorescence F_o ($F_m/F_o = 6.7$ in our leaves), and for the flash-induced fluorescence $F_f/F_o = 3.7$). Antenna fluorescence was emitted with the rate constant of 0.058 ns^{-1}, but the excitation was competitively quenched by internal thermal conversion and via intersystem crossing to the triplet state, with the total rate constant of 0.23 ns^{-1}. This rendered the excitation life-time in the antenna 3.5 ns and the absolute quantum yield for fluorescence emission 20%. Below we normalize calculated fluorescence yields in relation to this antenna yield, denoted $F_{max} = 1$.

Excitation hopping time in the antenna was joined with the radical pair formation time, resulting in the rate constant $ar = 6$ ns^{-1} for the formation of the radical pair from antenna excitation. The radical pair could recombine into the excited state, sending the excitation back to the antenna. In leaves, the "entropic force" of the large antenna resulted in 1:1 equilibration of the radical pair state with the excited antenna state—in absence of the electric field excitation spent a half of its lifetime in the antenna, the other half in the radical pair. Competitively with the radiative recombination, the radical pair could rapidly donate its electron to Q_A with the rate constant of 5 ns^{-1}. This rate constant determines the PSII photochemical quantum yield, found to be 0.65 in leaves (Laisk et al. 2014, see "Discussion"). Important was the role of the non-radiative recombination of the radical pair, quenching excitation in its non-fluorescent state. The corresponding rate constant of 2 ns^{-1} was chosen between the two exponentials reported in Schatz et al. (1987). Determined on the basis of integral fluorescence yields, these rate

constants for the one-RP model are generally faster than those used for the two-RP model by Lambrev et al. (2012) for the wild-type arabidopsis in the dark-adapted (no NPQ) state. Slower rate constant values resulted in too high F_o, not compatible with the measured F_m/F_o and F_f/F_o ratios.

In this model, electric field was assumed to exert counter-pressure on the radical pair state, increasing the radiative recombination rate as follows:

$$\frac{ra}{ar} = \exp\left(\frac{e\Delta E}{kT}\right), \quad (1)$$

where ar is the antenna → radical pair rate constant, but ra is the reverse rate constant, ΔE is the effective potential difference, V, T is absolute temperature (300 K in calculations), e is electron charge, C, and k is Bolzmann constant J K^{-1}. Increasing ΔE shifts the radical pair equilibrium towards the antenna, reducing the probability of the radical pair state and increasing the hopping time of excitation in the antenna—with this rising the fluorescence yield. In the F_m state, the 0.05 V potential difference increased the ra rate constant to 42 ns^{-1}.

Calculations were carried out with rate constants fitted to reproduce the excitation kinetics for three PSII states: open or the F_o state, Q_A reduced or the F_f state, and maximum fluorescence, F_m state (Fig. 8). In the panel, the ordinate scale unit directly shows the relative population of excited antennas and the photochemical quantum yield for open centers, but for fluorescence the antenna yield F_{max}, 0.2 in absolute units, is set to 1.0. Thus, the yields F_o, F_f and F_m are shown as a fraction of the theoretically possible maximum F_{max}—the condition when the radical pair state is not populated. The initial state for integration was set with excitation in the antenna, but Q_A oxidized, AeQo = 1 for the open state, and AeQr = 1 for the closed state. No more excitations were added during the excitation transfer process, while every open PSII proceeded through the states AeQo ↔ AgRQo → AgQr and every closed PSII proceeded through the states AeQr ↔ AgRQr ↔ AgQr. During the excitation transfer process, the running probability for fluorescence emission from the antenna was integrated with an aim to obtain the total fluorescence yield.

Navy blue curves in Fig. 8 indicate the open state. The fast-decaying dual-exponential curve shows how the excitation leaves the antenna. The rapidly increasing and then decaying curve, proceeding through the maximum of 0.25, shows population of the radical pair (initial 2 ns are enlarged in Fig. 8b). The upper curve saturating at 0.66 shows the time course of electron transfer to Q_A, but the lower curve saturating at 0.07 shows the fraction of excitations emitted as F_o fluorescence—in relation to the antenna yield of 0.2.

When the closed centers were calculated with $\Delta E = 0$ as the open centers were done, the F_f/F_o ratio of 3.7 was not obtained, but $\Delta E = 0.02$ V had to be assumed to reproduce

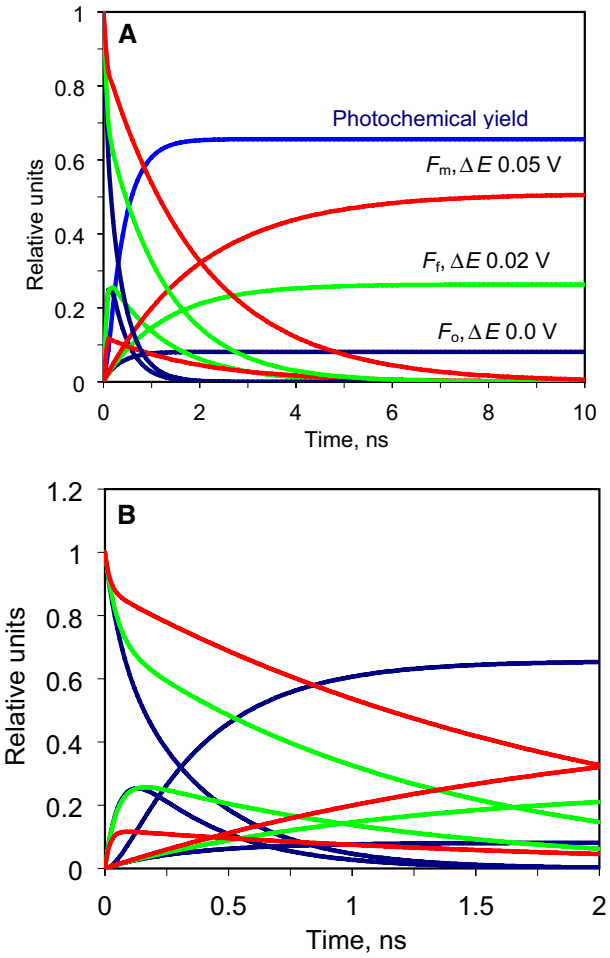

Fig. 8 Calculated time curves for excitation transfer for the three characteristic cases: open centers (blue lines), Q_A reduced centers (green lines) and membrane energized ($Q_A + Q_B$ reduced, red lines). Initially, antenna was excited in all centers (AeQo = 1), double-exponentially declining lines show the decay of antenna excitation; exponentially increasing is integrated fluorescence—for fluorescence the ordinate unit is yield from the antenna (20% absolute). For open centers, the photochemical yield 0.66 is calculated as the accumulating AgQr (Q_A reduced) fraction. For open centers, ΔE was 0, but increased as shown for Q_A reduced (F_f fluorescence) and $Q_A + Q_B$ reduced (membrane energized, F_m fluorescence) centers. For clarity panel B shows the initial 2 ns

the necessary F_f/F_o ratio (green curves). In this F_f state, excitation still rapidly equilibrates with the radical pair (initial fast decay of the antenna excitation), but the equilibrated state decays more slowly than with open centers. At its maximum, the radical pair state was populated in 0.25 of all PSII units.

To reach the F_m fluorescence yield, $\Delta E = 0.05$ V had to be assumed with closed centers (red curves). The initial equilibration between the antenna and the radical pair was as fast as in the F_f state, but the maximum population of the radical pair was only 0.12. In this state, the

fluorescence yield approached 0.5 of the antenna yield F_{max}—meaning that in the F_m state, the radical pair still quenched a significant part of excitations. The bi-exponential character of antenna excitation decay was still pronounced in the F_m state, though the amplitude of the fastest component was smaller than in the F_o and F_f states.

Discussion

Nature of the electric field

We showed that during a low to high light induction transient in sunflower leaves, Chl fluorescence of closed PSII units initially adjusted on a F_f yield at $F_f/F_o = 3.7$, but later during the induction increased to the F_m yield at $F_m/F_o = 6.7$. The F_f fluorescence level is similar to the ST flash-induced fluorescence level, typically 0.5–0.7 F_m (Joliot and Joliot 1964, 1977, 1981; Neubauer and Schreiber 1987; Samson and Bruce 1996). Such variability of fluorescence in closed PII is explainable in the framework of the antenna-radical pair excitation equilibrium model, based on very fast excitation transfer through the antenna and fast primary charge separation in PSII center Chls (Schatz et al. 1988; Akhtar et al. 2017). In this model, the antenna/radical pair excitation equilibrium constant has been found to be dependent on the open or closed state of the center. The mechanistic background of this dependence has been suggested to be a conformational relaxation processes in the protein. Though structurally the cation may rapidly move only between two radical pair states—from the D1 accessory Chl to the P_{D1} Chl—four different radical pair (RP) states have been postulated, to best fit the multi-exponential fluorescence decay curves (Szczepaniak et al. 2009). In this work, we generalized the "conformational relaxations" under the term "electric field" exerting counter-pressure on separated charges—considering that the ultimate reason for any change in electron energy must be an electric field.

Molecular nature of changes in the electric field penetrating deeply into the PSII center may be complex. In the presence of the ionophore valinomycin, inhibiting specifically the formation of membrane voltages, the magnitude of the secondary, J–I phase of fluorescence induction, was clearly diminished or was fully suppressed. The field-induced variation of fluorescence yield resulted mainly from the rate constant of primary charge separation, and to a smaller extent from the rate constant of charge recombination. The authors concluded that the light-driven formation of the thylakoid-membrane voltage results in an increase of the chlorophyll excited-state lifetime, a phenomenon explainable by the electric-field-induced shift of the free-energy level of the primary radical pair (Dau and Sauer 1992; Pospíšil and Dau 2002). The term photoelectrochemical quenching of Chl fluorescence was introduced by Vredenberg et al. (2009) to characterize the slow induction of fluorescence in pea leaves and isolated chloroplasts under low light intensities. Properties of this retarded slow rise, mainly suppression by low concentration of protonophores and responsiveness to complementary single-turnover flash excitation, suggested that the fluorescence increase during a train of 60 flashes was caused by release of a photo-electrochemical type of quenching, controlled by the trans-thylakoid proton pump powered by the light-driven Q-cycle. This suggests that a significant component of the PSII internal field is the overlapping delocalized transmembrane field, generated by electrochemical activity of the Q-cycle and PSI (Junge and Witt 1968). This field is rapidly generated during the dark–light induction of photosynthesis, but decreases later as the field component of membrane energization is replaced by proton concentration difference (Cruz et al. 2001; Klughammer et al. 2013; Lyu and Lazár 2017a, 2017b).

According to this assumption, no high F_m/F_o ratio could be expected with isolated PSII particles unable to energize the membrane. The F_f/F_o ratio was only 3–4 indeed when Q_A was reduced in oxygen-evolving photosystem II particles from *Synechococcus* by sodium dithionite (Schatz et al. 1987). However, in similar experiments, but using DCMU instead of sodium dithionite, a high ratio $F_m/F_o = 10$ was obtained (Szczepaniak et al. 2009). Similarly, in untreated leaves the flash-induced fluorescence yield is normally about 0.6 F_m (Joliot and Joliot 1964, 1977, 1981; Neubauer and Schreiber 1987; Samson and Bruce 1996), but the flash-induced F_f closely approaches F_m in DCMU-treated leaves (Schreiber and Krieger 1996; Schansker et al. 2011; Laisk and Oja 2013). After being driven into the F_m state, when a sunflower, pea or tobacco leaf was exposed to darkness during a few seconds, the florescence yield declined to a value of $2F_o$, but just one charge transfer was needed to return it to the F_m state again (Schansker et al. 2011; Laisk et al. 2015). This showed that while Q_A and Q_B both were reduced, Q_A could be oxidized in the dark, leaving Q_B occupied by PQH_2. Illumination of the leaf in this state was equivalent to the illumination of a DCMU-treated leaf, but PQH_2 occupying the Q_B site. As no membrane energization could be assumed in the PSII particles or DCMU-treated leaves, it suggests that the fluorescence yield of Q_A-reduced centers depends on the occupation of Q_B. The ST flash-induced fluorescence yield F_f is low when the flash is applied on open PSII—i.e. Q_A becomes reduced, though electron transport to Q_B is possible, but it did not occur yet. When electron transport from Q_A to Q_B is impossible—the Q_B site is occupied either by a plastoquinol or DCMU—then the transfer of just one electron is enough to reach the state close to F_m either in leaves (Schansker et al. 2011; Laisk and Oja 2013) or in PSII particles (Szczepaniak et al. 2009). Though the repulsive

electric field is the ultimate intrinsic reason causing variations in the antenna/radical pair equilibrium, the field may be enhanced by the delocalized transmembrane field, or it may be reconfigured by the occupation of the Q_B-binding site—whether electron transfer from Q_A to Q_B is possible or is not possible (Prášil et al. 2018).

Interestingly, a stepwise increase of fluorescence in response to a train of ST flashes was recently detected in DCMU-inhibited PSII core complexes isolated from *Thermosynechococcus vulcanus* (Sipka et al. 2019). High Chl fluorescence with the maximum F_v/F_m parameter 0.85 could only be induced by a train of the flashes. As no PSI and Q-cycle activity was present in the isolated PSII core complexes, membrane energization did not occur—unless PSII itself was electrochemically active (Laisk et al. 2015). Or more likely, in the isolated complexes PQH_2 could spread within a membrane volume before it significantly accumulated in the Q_B sites.

Amplitude of F_m/F_o

The model defines two extreme values of the fluorescence yield: the minimum is F_o, emitted by excitation in the antenna, reversibly equilibrated with the radical pair state while the latter is quenched by photochemical charge transfer and non-radiative recombination. The theoretical maximum is the antenna fluorescence F_{max}—when the repulsive electric field is so strong that the radical pair practically cannot exist. Experimental cases may cover the span between these extremes. Our model placed the F_m fluorescence yield at a half-way between F_o and the antenna yield of 0.2, normalized to unity in Fig. 8.

The rate constants for our model were chosen by fitting the integral fluorescence yields F_o, F_f and F_m and considering the measured quantum yield of PSII photochemistry, as described in the Model section. Though the fluorescence decay curves were not available for our leaves, nevertheless our rate constants are close to those derived from time-resolved measurements for wild-type arabidopsis (Lambrev et al. 2012), though still somewhat faster—it was necessary to fit the low F_o yield. The position of F_m between F_o and F_{max} was determined considering reported fluorescence lifetimes. A typical fluorescence lifetime in isolated light-harvesting antenna complexes is 3.5 ns (Pascal et al. 2005; Gruber et al. 2015). In leaves, the average lifetime in the F_m state does not exceed 2 ns (Belgio et al. 2012), reported to be 1.3 ns in *Arabidopsis* (Holzwarth et al. 2009), 0.9 ns in maize (Chukhutsina et al. 2019) or 0.7 ns in thylakoid membranes (Farooq et al. 1918). This quite clearly shows that in the F_m state, the radical pair is not completely gated for the entrance of excitation, but the F_m fluorescence is still significantly quenched by non-radiative recombination within the radical pair. The conclusion is confirmed by fluorescence decay curves. Our modelled decay curves were multi-exponential when the radical pair was populated, but termination of excitation in the antenna—the F_{max} level—was described by a single rate constant, as experimentally confirmed in an individual LHCII (Gruber et al. 2015) and LHCII trimers (Pascal et al. 2005). In accordance with this, our model reproduced a single exponent for the F_{max} state, but at the F_m state the modeled decay curves still remained bi-exponential.

Relationship between Chl fluorescence and photochemistry

Fluorescence has been found to be a convenient signal, proportional to light energy *not* used by photosynthesis. A wide-spread understanding of fluorescence is based on a simple model, assuming that several processes are simultaneously competing to terminate (quench) an excitation. The corresponding formula for fluorescence yield F is

$$F_o = \frac{k_f}{\left(k_f + k_d + k_p\right)} \tag{2}$$

where k are the competing rate constants with subscripts f for fluorescence emission, d for thermal dissipation and p for the photochemical process. Fluorescence yield is minimal, F_o, when all the competitive quenchers are active, but the yield is much higher, F_m, when photochemistry is blocked ($k_p = 0$). Considering that the yield of photochemistry is expressed as

$$Y_p = \frac{k_p}{\left(k_f + k_d + k_p\right)}, \tag{3}$$

the following equation relating the photochemical yield Y_p to the measurable fluorescence yields was derived (Genty et al. 1989)

$$Y_p = \frac{F_m - F_o}{F_m}. \tag{4}$$

Inserting the calculated F_o and F_m (Fig. 8) into Eq. (4) we obtain the photochemical yield $Y_p = 0.85$, which is by far higher than the model/calculated yield 0.66. Using the flash-induced F_f instead of F_m in Eq. (4), the yield would be $Y_p = 0.72$.

These yield calculations assume that the dissipative quenchers k_d are constantly present, independent of the presence or absence of photochemistry, k_p. Experimentally, the F_m yield is determined after all PSII centers are closed due to complete reduction of the whole electron transport chain under a strong "saturation" light pulse, but F_o is determined either in the dark or under very low light—generally, under conditions facilitating complete oxidation of the PSII electron acceptors, including Q_B. Our present results show that

the photochemical act takes place in the state when fluorescence of closed centers is much lower than in the final F_m state. The flash-induced F_f is closer to the fluorescence of closed centers at the moment of electron transfer to Q_A, but even it may be somewhat overestimated: we needed to assume an additional membrane voltage of 0.02 V in order to model the measured F_f/F_o ratio. For this same reason, Eq. (4) resulted in the quantum yield of 0.72 when F_f was inserted, but not 0.66 as calculated from the model.

In leaves, the total quantum yield of photosynthesis has been reported to be 0.106 O_2 evolved per photon absorbed (Ehleringer and Björkman 1977), but this does not characterize the PSII yield, as partitioning of excitation between PSII and PSI was not known. The usually assumed even partitioning would mean 0.212 O_2 or 0.85 electrons transferred per PSII photon. A more detailed spectral study of the quantum yields of PSII and PSI together with excitation partitioning between the photosystems in sunflower leaves (Laisk et al. 2014) revealed the global yield of the two photosystems of 0.72 in the red part of spectrum. After the yields were partitioned, the PSI yield $y_I = 0.88$, but unexpectedly this photosystem absorbed only about 1/3 of all quanta; consequently, about 2/3 of the quanta were absorbed by PSII, but processed with the low intrinsic yield $y_{II} = 0.63$. Such a low PSII quantum yield was incompatible with the high $(F_m - F_o)/F_m$ value in these same sunflower leaves, but is consistent with the present notion that excitation is additionally lost in the state of the $Pheo^-P680^+$ radical pair, which can be non-radiatively recombined before the electron is transferred to Q_A. In our model, the rate constants were chosen considering this relatively low-PSII photochemical yield.

Concluding this section, the common fluorescence-based calculations of the quantum yield of PSII photochemistry overestimate the PSII quantum yield for two reasons. First, excitation is competitively quenched not only in the antenna but also in the radical pair, not observable in fluorescence. Second, F_m is significantly overestimated when measured in the state of the maximum membrane voltage—just after the whole electron transport chain became reduced. Though not fully correct, but a better approximation would be to use the flash-induced F_f value instead of F_m, as the former is less overestimated than the latter.

General conclusions

The antenna/radical pair equilibrium theory predicts that fluorescence yield of a closed (acceptor reduced) photochemical center may vary dependent on energetic depth of the radical pair trap and on probability for non-radiative recombination of the radical pair. A spectacular example of the deep radical pair trap is photosystem I, where the trapped excitation returns to the antenna with a very low probability, even if further electron transport is blocked by a reduced acceptor (Croce et al. 2000; Gobets and van Grondelle 2001). For example, in sunflower leaves, the room-temperature 750 nm fluorescence yield from PSI was found to be 37% of F_o (Peterson et al. 2014), not variable over the whole induction trace, during which P700 transiently became oxidized and finally reduced again. This result is consistent with the model proposed by (Holzwarth et al. 2006), assuming the "accessory" Chl is the primary electron donor, but not P700.

In PSII the relaxed $Pheo^-P680^+$ radical pair is shallow, in open centers resulting in about double higher F_o than in PSI. In leaves, the entropic force of the large antenna contributes, resulting in even, 1:1 equilibration of excitation between the antenna and the radical pair. Thanks to the shallow trap, a low additional electric field of 0.05 V increases the fluorescence yield of closed reaction centers more than two times, efficiently converting the trap into a small bump.

The central notion from this work is the cooperative allosteric effect between PSII: after an electron has been carried through the membrane in a local PSII center, a delocalized cooperative force is generated, counteracting the presence of the primary radical pair in *adjacent* centers. As discussed above, the intrinsic nature of the force is electric field anyway, but its origin may be related just to reorganization of the PSII internal field dependent on the occupation of the Q_B site, or the effect may be more complex, involving a component exerted by delocalized transmembrane electric field—termed membrane energization (Bulychev and Vredenberg 1999). The high fluorescence of DCMU-poisoned samples speaks for the internal, protein conformation relaxation, but systematic studies (Dau and Sauer 1992; Pospíšil and Dau 2002; Vredenberg et al. 2009), emphasizing the role of membrane energization, cannot be ignored. The cooperative character of the delocalized transmembrane field is easily understandable. Plastoquinol also acts cooperatively, because PQH_2 generated by still open centers may bind into the Q_B pockets of adjacent centers—particularly well if PQH_2 has strong product-inhibitory affinity to the Q_B pocket (Laisk and Oja 2018). But the problem is, can an electron transfer from $Pheo^-$ to Q_A—what happens during a ST flash in a PSII center—allosterically influence the internal electric field within adjacent PSII centers?

Though the intrinsic mechanism may need elaboration, we have experimentally shown that fluorescence yield of closed PSII centers does increase during a low to high light induction—while the membrane gets energized and the plastoquinone pool gets reduced. During the very initial part of the induction, while electrons were transferred within the PSII, our data showed a constant fluorescence yield, similar to the post-flash fluorescence yield F_f. As our induction traces were started not from the dark but from a low light intensity (in order to randomize the S-states), the whole electron transport chain was already energized—to the extent necessary to support ATP synthesis at the low

rate. Therefore, our data do not cover the completely de-energized state, comparable to the time-resolved fluorescence experiments. For understanding of the PSII electron transport process it would be necessary to know, is there a cooperative influence between PSII when electrons are moved only within the center? The term "protein conformational relaxation processes" (Szczepaniak et al. 2009) may have a wider content than temporal reorganization of protein conformation within a PSII center, proceeding simultaneously with Chl excitation decay.

Acknowledgement We appreciate constructive discussions with Alfred Holzwarth, facilitating formulation of conclusions.

Funding The project was financed by University of Tartu (Basic funding), Institute of Technology, and by Estonian Academy of Science (A.L.).

Compliance with ethical standards

Conflict of interest The authors declare that they have no conflict of interest.

References

Akhtar P, Zhang C, Do TN, Garab G, Lambrev PH, Tan H-S (2017) Two-dimensional spectroscopy of chlorophyll a excited-state equilibration in light-harvesting complex II. J Phys Chem Lett 8:257–263

Belgio E, Johnson MP, Jurić S, Ruban AV (2012) Higher plant photosystem II light-harvesting antenna, not the reaction center, determines the excited-state lifetime—both the maximum and the non-photochemically quenched. Biophys J 102:2761–2771

Bulychev AA, Vredenberg WJ (1999) Light-triggered electrical events in the thylakoid membrane of plant chloroplasts. Physiol Plant 105:577–584

Chukhutsina VU, Holzwarth AR, Croce R (2019) Time-resolved fluorescence measurements on leaves: principles and recent developments. Photosynth Res 140:355–369

Croce R, Dorra D, Holzwarth AR, Jennings RC (2000) Fluorescence decay and spectral evolution in intact photosystem I of higher plants. Biochemistry 39:6341–6348

Cruz JA, Sacksteder CA, Kanazawa A, Kramer DM (2001) Contribution of electric field (DY) to steady-state transthylakoid proton motive force (*pmf*) in vitro and in vivo. Control of *pmf* parsing into DY and DpH by ionic strength. Biochemistry 40:1226–1237

Dau H, Sauer K (1992) Electric field effect on the picosecond fluorescence of Photosystem II and its relation to the energetics and kinetics of primary charge separation. Biochim Biophys Acta 1102:91–106

Delosme R (1967) Étude de l'induction de fluorescence des algues vertes et des chloroplastes an début d'une illumination intense. Biochim Biophys Acta 143:108–128

Ehleringer J, Björkman O (1977) Quantum yields for CO_2 uptake in C_3 and C_4 plants. Dependence on temperature, CO_2 and O_2 concentration. Plant Physiol 59:86–90

Farooq S, Chmeliov J, Wientjes E, Koehorst R, Bader A, Valkunas L, Trinkunas G, van Amerongen H (1918) Dynamic feedback of the photosystem II reaction centre on photoprotection in plants. Nature Plants 4:225–231

Genty B, Briantais JM, Baker NR (1989) The relationship between quantum yield of photosynthetic electron transport and quenching of chlorophyll fluorescence. Biochim Biophys Acta 990:87–92

Gobets B, van Grondelle R (2001) Energy transfer and trapping in photosystem I. Biochim Biophys Acta 1507:80–99

Gruber JM, Chmeliov J, Krüger TPJ, Valkunas L, van Grondelle R (2015) Singlet–triplet annihilation in single LHCII complexes. Phys Chem Chem Phys 17:19844–19853

Holzwarth AR, Müller MG, Niklas J, Lubitz W (2006) Ultrafast transient absorption studies on Photosystem I reaction centers from *Chlamydomonas reinhardtii*. 2: Mutations near the P700 reaction center chlorophylls provide new Insight into the nature of the primary electron donor. Biophys J 90:552–565

Holzwarth AR, Miloslavina Y, Nilkens M, Jahns P (2009) Identification of two quenching sites active in the regulation of photosynthetic light-harvesting. Chem Phys Lett 483:262–267

Joliot A, Joliot P (1964) Étude cinétique de la réaction photochimique libérant l'oxygène au cours de la photosynthése. C R Acad Sci Paris 258:4622–4625

Joliot P, Joliot A (1977) Evidence for a double hit process in photosystem II based on fluorescence studies. Biochim Biophys Acta 462:559–574

Joliot P, Joliot A (1981) Double photoreactions induced by laser flash as measured by oxygen emission. Biochim Biophys Acta 638:132–140

Junge W, Witt T (1968) On the ion transport system of photosynthesis. Investigations on a molecular level. Z Naturforsch 23b:244–254

Keuper HJK, Sauer K (1989) Effect of photosystem II reaction center closure on nanosecond fluorescence relaxation kinetics. Photosynth Res 20:85–103

Klughammer K, Siebke K, Schreiber U (2013) Continuous ECS-indicated recording of the proton-motive charge flux in leaves. Photosynth Res 117:471–487

Koblížek M, Kaftan D, Nedbal L (2001) On the relationship between the non-photochemical quenching of the chlorophyll fluorescence and the photosystem II light harvesting efficiency. A repetitive flash fluorescence induction study. Photosynth Res 68:141–152

Laisk A, Oja V (2013) Thermal phase and excitonic connectivity in fluorescence induction. Photosynth Res 117:431–448. https://doi.org/10.1007/s11120-013-9915-1

Laisk A, Oja V (2018) Kinetics of photosystem II electron transport: a mathematical analysis based on chlorophyll fluorescence induction. Photosynth Res 136:63–82. https://doi.org/10.1007/s11120-017-0439-y

Laisk A, Oja V, Rasulov B, Rämma H, Eichelmann H, Kasparova I, Pettai H, Padu E, Vapaavuori E (2002) A computer-operated routine of gas exchange and optical measurements to diagnose photosynthetic apparatus in leaves. Plant Cell Env 25:923–943

Laisk A, Eichelmann H, Oja V (2012) Oxygen evolution and chlorophyll fluorescence from multiple turnover light pulses: charge recombination in photosystem II in sunflower leaves. Photosynth Res 113:145–155

Laisk A, Oja V, Eichelmann H, Dall'Osto L, (2014) Action spectra of photosystems II and I and quantum yield of photosynthesis in leaves in State 1. Biochim Biophys Acta 1837:315–325

Laisk A, Eichelmann H, Oja V (2015) Oxidation of plastohydroquinone by photosystem II and by dioxygen in leaves. Biochim Biophys Acta 1847:565–575

Lambrev PH, Miloslavina Y, Jahns P, Holzwarth AR (2012) On the relationship between non-photochemical quenching and photoprotection of Photosystem II. Biochim Biophys Acta 1817:760–769

Leibl W, Breton J, Deprez J, Trissl H-W (1989) Photoelectric study on the kinetics of trapping and charge stabilization in oriented PS II membranes. Photosynth Res 22:257–275

Lyu H, Lazár D (2017a) Modeling the light-induced electric potential difference ($\Delta\Psi$), the pH difference (ΔpH) and the proton motive

force across the thylakoid membrane in C_3 leaves. J Theor Biol 413:11–23

Lyu H, Lazár D (2017b) Modeling the light-induced electric potential difference ΔΨ across the thylakoid membrane based on the transition state rate theory. Biochim Biophys Acta 1858:239–248

Neubauer C, Schreiber U (1987) The polyphasic rise of chlorophyll fluorescence upon onset of strong continuous illumination: I. Saturation characteristics and partial control by the photosystem II acceptor side. Z Naturforschung 42c:123–131

Oja V, Eichelmann H, Anijalg A, Rämma H, Laisk A (2010) Equilibrium or disequilibrium? A dual-wavelength investigation of photosystem I donors. Photosynth Res. https://doi.org/10.1007/s11120-010-9534-z

Pascal AA, Liu Z, Broess K, van Oort B, van Amerongen H, Wang C, Horton P, Robert B, Chang W, Ruban A (2005) Molecular basis of photoprotection and control of photosynthetic light harvesting. Nature 436:134–137. https://doi.org/10.1038/nature03795

Peterson RB, Oja V, Eichelmann H, Bichele I, Dall'Osto L, Laisk A (2014) Fluorescence F_0 of photosystems II and I in developing C_3 and C_4 leaves, and implications on regulation of excitation balance. Photosynth Res 122:41–56

Pospíšil P, Dau H (2002) Valinomycin sensitivity proves that light-induced thylakoid voltages result in millisecond phase of chlorophyll f luorescence transients. Biochim Biophys Acta 1554:94–100

Prášil O, Kolber ZS, Falkowski PG (2018) Control of the maximal chlorophyll fluorescence yield by the Q_B binding site. Photosynthetica 56:150–162

Samson G, Bruce D (1996) Origin of the low yield of chlorophyll fluorescence induced by single turnover flash in spinach thylakoids. Biochim Biophys Acta 1276:147–153

Schansker G, To'th S, Kova'cs L, Holzwarth AR, Garab G (2011) Evidence for a fluorescence yield change driven by a light-induced conformational change within photosystem II during the fast chlorophyll a fluorescence rise. Biochim Biophys Acta 1807:1032–1043

Schatz G, Brock H, Holzwarth AR (1987) Picosecond kinetics of fluorescence and absorbance changes in photosystem II particles excited at low photon density. Proc Natl Acad Sci USA 84:8414–8418

Schatz GH, Brock H, Holzwarth AR (1988) Kinetic and energetic model for the primary processes in photosystem II. Biophys J 54:397–405

Schreiber U (2002) Assessment of maximal fluorescence yield. Donor-side dependent quenching and QB-quenching. In: Kooten O, Snel J (eds) Plant Spectrophotometry: Applications and Basic research. Rozenberg, Amsterdam, pp 23–47

Schreiber U, Krieger A (1996) Two fundamentally different types of variable chlorophyll fluorescence in vivo. FEBS Lett 397:131–135

Schreiber U, Neubauer C (1987) The polyphasic rise of chlorophyll fluorescence upon onset of strong continous illumination: II. Partial control by the photosystem II donor side and possible ways of interpretation. Z Naturforsch 42c:132–141

Schreiber U, Neubauer C (1990) O_2-dependent electron flow, membrane energization and the mechanism of non-photochemical quenching of chlorophyll fluorescence. Photosynth Res 25:279–293

Sipka G, Müller P, Brettel K, Magyar M, Kovács L, Zhu Q, Xiao Y, Han G, Lambrev PH, Shen J-R, Garab G (2019) Redox transients of P680 associated with the incremental chlorophyll-a fluorescence yield rises elicited by a series of saturating flashes in diuron-treated photosystem II core complex of *Thermosynechococcus vulcanus*. Physiol Plantarum 166:22–32

Stirbet A, Govindjee (2012) Chlorophyll a fluorescence induction: a personal perspective of the thermal phase, the J-I-P rise. Photosynth Res 113:15–61

Szczepaniak M, Sugiura M, Holzwarth AR (2008) The role of TyrD in the eelctron transfer kinetics in photosystem II. Biochim Biophys Acta 1777:1510–1517

Szczepaniak M, Sander J, Nowaczyk M, Müller MG, Rögner M, Holzwarth AR (2009) Charge separation, stabilization, and protein relaxation in photosystem II core particles with closed reaction center. Biophys J 96:621–631

Vredenberg WJ (2008) Analysis of initial chlorophyll fluorescence induction kinetics in chloroplasts in terms of rate constants of donor side quenching release and electron trapping in photosystem II. Photosynth Res 96:83–97

Vredenberg W, Durchan M, Prášil O (2009) Photochemical and photoelectrochemical quenching of chlorophyll fluorescence in photosystem II. Biochim Biophys Acta 1787:1468–1478